eJSE International

*Electronic Journal of Structural Engineering 18(2) 2018*

# Experimental and Numerical Investigation of an Eccentrically Loaded Strip Footing on Reinforced Sand Slope

A. Abdi*, K. Abbeche, R. Boufarh, and B. Mazouz

*Department of Civil Engineering, Faculty of Technology, University of Batna 2, Algeria*

* Email: abdiabdelmadjid14@gmail.com

ABSTRACT: An experimental program and numerical computations were performed to investigate the slope effect on the bearing capacity of an eccentrically loaded strip footing. Two cases were considered: unreinforced sand slope and reinforced slope by geogrid. Tests were conducted on scaled footing models under various eccentric loads. A parametric study was carried out to examine the effect of the slope on the bearing capacity and the depth of geogrid layers under different eccentric loads. It was shown that the location of the eccentricity of applied load with respect to the slope face has a significant effect on the bearing capacity. This latter increase when the distance from applied eccentric load to the slope face also increases. Obtained results also showed that the bearing capacity of strip footing also depends on the inclination of ground surface in comparison to that predicted from horizontal ground.

KEYWORDS: Eccentricity, Slope, Towards, Far away, footing, reinforced, sand.

## 1 INTRODUTION

In civil engineering, the foundations can be sometimes subjected to eccentric or/and inclined loads, if a foundation is subjected to lateral loads and moments in addition to vertical loads, eccentricity in loading results. The basic problem is to determine the effect of the eccentricity on the ultimate bearing capacity of the foundation. When a foundation is subjected to an eccentric vertical load the contact pressure increases on the side of eccentricity and decreases on the opposite side [1]. The bearing capacity of an eccentrically loaded footing maybe determined using the concept of useful (or effective) width proposed by Meyerhof [2], and it has been widely accepted in geotechnical design. The form of bearing capacity factors $N_\gamma$, $N_q$, and $N_c$ of an eccentrically loaded footing is determined by analytical formulation. It be assumed that the rupture surface is a log spiral, and failure occurs on the same side as the eccentricity with respect to the center of the footing [3]. In addition to the load eccentricity, when a shallow foundation is placed on top of slope and subjected to axial load, its bearing capacity is reduced as compared to that of footing on horizontal ground [4]. In the last decades extensive studies have been made for two dimensional problems of a strip footing resting on a horizontal or inclined slope surface so that different methods of analysis are available [5-8]. Unfortunately, there are few studies on the combined effect of load eccentricity and slope on bearing capacity. Saran and Reddy [9] suggested the form of the bearing capacity formula using a limit equilibrium approach. Cure, Turker [10] studied the effect of the ultimate load of the footings near slopes. They conducted a series of laboratory model tests of a strip footing resting on a sand slope and subjected to eccentric load. The ultimate loads decreased as the eccentricity increased. This decrease is due to the combination of eccentricity and slope. The $N_\gamma$ and $N_q$ coefficients follow similar trends and negatively correlate with e/B. In recent years, due to ease of use and ability to improve bearing capacity of footings under static loads, geosynthetics reinforced soil has been widely of interest to geotechnical engineers in various applications [11-18]. For the eccentrically loaded foundations placed on horizontal soil there is geometrical symmetry for the footing center, however in the case of non-horizontal soil (slope) this symmetry is lost and there are two cases of loading, the first is eccentric load located on the side towards the slope face and the second is the eccentric load located on the opposite side far away from the slope face (Fig. 1).

Al-Jubair and Abbas [19] have numerically studied the effects of variation in footing closeness, loading eccentricity and slope angle of a strip footing constructed near the edge of a sloping cohesive ground. They found that the slope effect diminishes as the footing distance from the edge approaches (1.5) times its width. Turker et al [20] conducted a series of bearing capacity tests with an eccentrically loaded model surface and shallow strip footings resting close to reinforced sand slopes to investigate ultimate loads, failure surfaces, load–displacement

curves, rotation of footing. The results indicate that ultimate loads decreased with increasing eccentricity. This decrease is due to a combination of eccentricity and slope. The use of geotextile reinforcement increased ultimate loads in comparison with unreinforced cases. Failure surfaces were not symmetrical, primary failure surfaces developed on the eccentricity (slope) side, and secondary failure surfaces developed on the other side. Lengths of failure surfaces decreased with increasing eccentricity. Prior to failure, footings always rotated towards the eccentricity (slope) side a few degrees. In this work, the ultimate load capacity of an eccentrically loaded surface and shallow strip footing close to a reinforced sand slope, such as failure surfaces, load displacement curves of footings were tested experimentally. Thus, the effect of load eccentricity location relative to the slope face on bearing capacity of strip footings on the reinforced sand slope was examined.

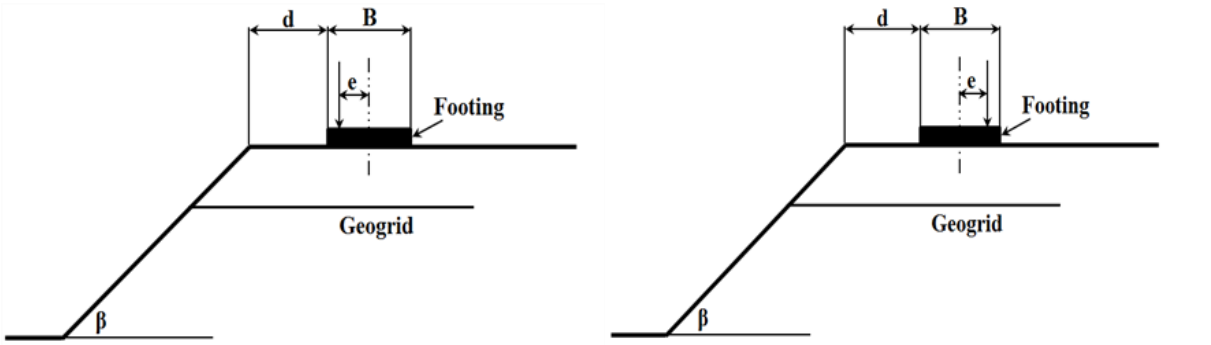


Figure 1 - load eccentricity location relative to the slope face

## 2 EXPERIMENTAL MODEL TEST

### *2.1 Test program and description*

The load tests were conducted in a rigid steel test tank with inside dimensions 1500×500×600mm. one of the tow sidewalls of tank was prepared with a thick and transparent glass to observe the failure mechanism during the tests.

Horizontal and inclined lines were marked on the glass to control the sand layers and the slope geometry. The plane strain condition is ensured by building the test tank sufficiently rigid. The loading process consists a rigid beam steel used as a lever mechanism. Load was applied through a weights putted on the lever and measured by using load sensor (15 kN) and displacements were measured by dial gauge placed at the point of load application on the footing. A schematic view of the test configuration with the symbols used in this study is illustrated in Fig. 2.

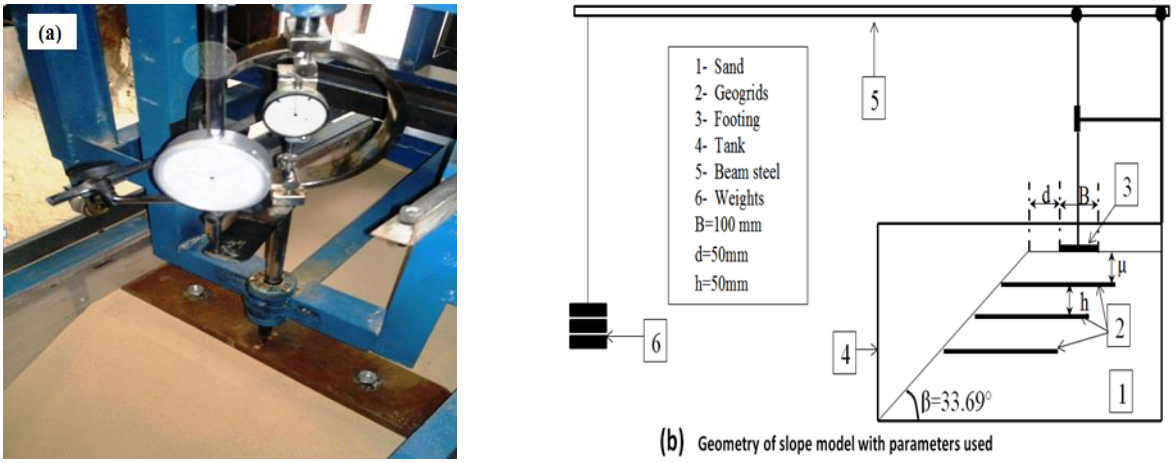


Figure 2 -Schematic view of the model test

The footing model was placed in the tank at a distance 50 mm to the slope crest, with the length of the footing parallel to the width of the tank. The side wall friction effects on the model test results were reduced by making the two ends of footing smooth. A layer of sand paper is cemented on the base of the footing model with epoxy glue to make it rough. Numerous holes were created on the upper side of the footing plate so that different eccentricities, e = 0, 10, 20, 30 mm or e/B = 0, 0.1, 0.2, 0.3) can be applied (Fig. 3).

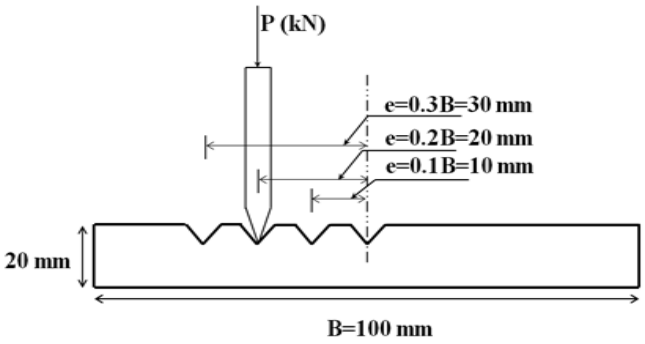


Figure 3 -Footing model with eccentricities

The sand used in the experimental investigation was dry pit sand with coefficient of uniformity ($C_u$) of 3.08 and coefficient of curvature ($C_c$) of 1.29. The maximum and minimum dry unit weights of the tested sand are found to be 19.3 and 14.1 kN/m$^3$. The average unit weight and relative density achieved in the test tank using a sand raining technique in all tests of sand was kept at 16.2 kN/m$^3$ and 60%. The particle size distribution was characterized using the dry sieving method and the results are shown in Fig. 4. The internal friction angle of compacted sand at relative density of 60% measured from a series of direct shear tests is approximately 38°. Other parameters of the tested sand are illustrated in Table 1.

A commercially uniaxial geogrid, made from transparent polyester (PET R6 80/20) was used as reinforcement element. The maximum tensile strength of the geogrid was found to be 56 kN/m. The geogrid mesh aperture size is 30 × 73 mm. Other properties are given in Table 2.

Table 1- Material properties of the sand used

| **parameter** | Cohesion C (kPa) | Angle of internal friction (°) | Unit weight, γ (kN/m$^3$) | Maximum dry density (kN/m$^3$) | Minimum dry density (kN/m$^3$) | D10 (mm) | D30 (mm) | D60 (mm) | Coefficient of uniformity, Cu | Coefficient of curvature, Cc |
|---|---|---|---|---|---|---|---|---|---|---|
| **Value** | 0.0 | 38 | 16.2 | 19.3 | 13.92 | 0.12 | 0.37 | 0.24 | 3.08 | 1.29 |

Table 2- Properties of the geogrid

| Raw material | Surface ground (g/m$^2$) | Resistance to traction (kN/m) | Elongation (%) | Resistance to the traction for 1% of elongation (kN/m) | Resistance to the traction for 5% of elongation (kN/m) | meshes Opening (mm×mm) | Elongation before service (%) | rollers Dimension, length and width (m×m) |
|---|---|---|---|---|---|---|---|---|
| (PET) | 380 | 20≤ RT ≤ 80 | 20≤ ΔL ≤ 80 | 16 | 56 | 73×30 | 0 | 4.75×100 |

## *2.2 Preparation of slope*

The procedure adopted for the reinforced model slope construction was the same as those experienced by Choudhary, Jha [21]. The dry sand was filed and compacted into the tank in ten equal layers each 50 mm thick in order to ensure uniform compaction of each layer. In case of reinforced sand slope, the reinforcement was placed at the desired depth within the fill (single layer as well for multiple layers; as the case may be) and the compaction was then continued in a similar manner until the desired height was reached. The length of reinforcement was kept constant ($L_R$=0.6 m) throughout all tests model and at any given position the location of the reinforcement was such that it extended up to the face of the slope. After that; the compacted sand bed was dug carefully to achieve the desired slope, then the straight face of the slope has been leveled by a rigid metal rule. Each series was conducted to study the effect of one parameter while the other variables were remaining constant. The varied conditions include the load eccentricity location relative to the slope face, the number of geogrid layers (N) and depth to topmost layer of geogrid (μ). Table 3 shows the test setup conducted for this study. The testing program for load eccentricity located on the side towards the slope face considered positive (+) was also similar to that for load eccentricity located on the other side far away from the slope face considered negative (-).

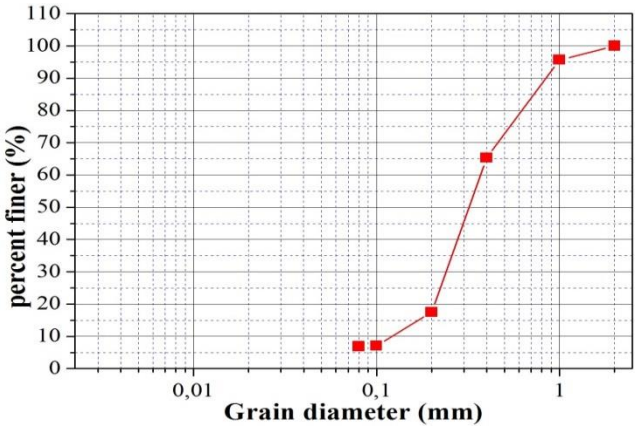


Figure 4 -Particle size distribution curve for the tested sand

Table 3- Program tests setup

| Test ref | N | e/B | μ/B | d/B | tg(β) |
|---|---|---|---|---|---|
| 00 | 0 | 0 | | 0.5 | 2/3 |
| 01 | | 0.1 | | | |
| 02 | | 0.2 | | | |
| 03 | | 0.3 | | | |
| 1025; 1050; 1075 | 1 | 0 | 0.25 | | |
| 2025; 2050; 2075 | 2 | | 0.5 | | |
| 3025; 3050; 3075 | 3 | | 0.75 | | |
| 1125; 1150; 1175 | 1 | 0.1 | 0.25 | | |
| 2125; 2150; 2175 | 2 | | 0.5 | | |
| 3125; 3150; 3175 | 3 | | 0.75 | | |
| 1225; 1250; 1275 | 1 | 0.2 | 0.25 | | |
| 2225; 2250; 2275 | 2 | | 0.5 | | |
| 3225; 3250; 3275 | 3 | | 0.75 | | |
| 1325; 1350; 1375 | 1 | 0.3 | 0.25 | | |
| 2325; 2350; 2375 | 2 | | 0.5 | | |
| 3325; 3350; 3375 | 3 | | 0.75 | | |

## 3 NUMERICAL STUDY

The analysis was developed using a two-dimensional plane-strain elasto-plastic finite element computer program Plaxis 2D [22], 2002). The computer program was conducted based on the assumptions that the foundation soil behaved as a non-linear elastic—perfectly plastic material. The geometry of the typical finite element model adopted for the analysis is the same as the experimental model. The left vertical line of the model was constrained horizontally, and the bottom horizontal boundary was constrained in both the horizontal and vertical directions. The interaction between the geogrid and the soil was simulated by interface elements located between the reinforcement and the soil surfaces. The interface between the contacts surfaces were modeled by a suitable value for the strength reduction factor at the interface compared with the corresponding soil strengths.

The adopted soil parameters were assumed to remain the same as in the laboratory tests in all the finite element analyses for the unreinforced system. Strip footing was simulated by creating a rectangular region and using a linear elastic material model. For the reinforced case, a reinforcement layer was introduced at the required depth with appropriate strength reduction factors. To obtain good results of numerical simulation, it is necessary to adopt a right materiel to simulate the reinforcement and soil reinforcement interaction [23].

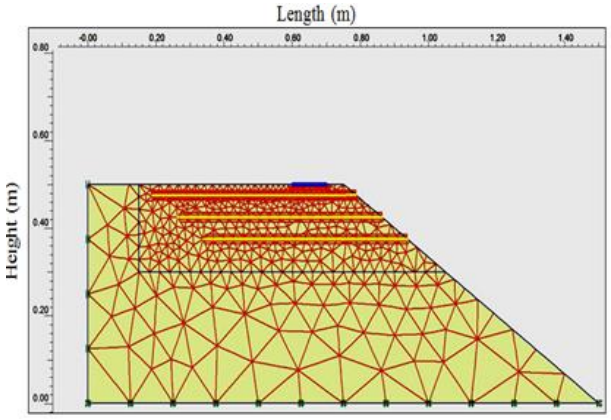


Figure 5 -Numerical model test with mesh size

The geogrid reinforcement was simulated with a five-node bar element by using the geogrid option of Plaxis 2D. A 15-node triangle plain strain element

was used to create the finite-element mesh. The Mohr Coulomb model was used to simulate the behavior of sand. The Mohr–Coulomb model requires a total of five parameters, which are listed as Poisson's ratio, cohesion, friction angle, Young's modulus and dilatancy angle. The Poisson's ratio of the sand was accepted as 0.20, based on the recommendation for medium density sand from Kumar and Ilamparuthi [4]. The materiel parameters for the numerical model parameters are illustrated in Table 4. Due to the stress con-centration around the foundation, the mesh size was locally refined in these regions (Fig. 5). The initial conditions generally comprise the initial groundwater conditions, the initial geometry configuration, and the initial effective stress state. The sand layer was dry, which made implementing ground water condition unnecessary. The initial stress condition of the slope was generated by applying the gravity force characterized by the soil unit weight including the geogrid reinforcements.

Table 4- Materiel properties for the numerical model

| Materiel | Materiel model | $\gamma_{unsat}$(kN/m$^3$) | $\gamma_{sat}$ (kN/m$^3$) | E (kPa) | ν | EA | EI | φ(°) | ψ(°) | R |
|---|---|---|---|---|---|---|---|---|---|---|
| Sand | Mohr-Coulomb | 16.2 | 19.35 | 12000 | 0.2 | | | 38 | 6 | 0.7 |
| Geogrid | | | | | | 500 | 1.75E+03 | | | |
| Foundation | | | | | | | 2.10E+07 | | | |

## 4 RESULTS AND DISCUSSION

A total of 70 bearing capacity tests were carried out by using a model strip footing on reinforced and unreinforced sand. Three different eccentricities (e/B=0, e/B=0.1, 0.2, e/B=0.3) located on the side towards the slope face, and the same eccentricities located on the opposite side far away from the slope face were applied to a model footing. Thus, the effects of eccentricity on load–settlement and failure mechanism were obtained and evaluated. Load–settlement relations obtained from experimental investigation are shown in Fig. 6. The tangent intersection method, suggested by Trautmann and Kulhawy [24] was used to estimate the ultimate bearing capacity for each model test. For the case of unreinforced sand the curves and the failure loads for the case of the negative eccentricities are superior to those for the case of the positive eccentricities (Fig. 6 (a)). The obtained results of the laboratory tests demonstrates that the load eccentricity and its relative location to the slope face has a significant effect on the ultimate bearing capacity .The ultimate bearing capacity increases as the load eccentricity decreases in both cases of negative and positive eccentricity. The results of this experimental work are close to the results reported by Saran and Reddy [9] and Cure, Turker [10]. When the primary failure surface becomes wide and deep, the ultimate bearing capacity of the tested strip footing increases from the slope side beneath the footing. A much greater pressure is therefore needed to the failure surface to reach the slope. The results in the case of reinforced sand have shown that for strip footing loaded by small negative load eccentricity (e/B=-0.1), the bearing capacity becomes greater than that of the same footing subjected to a centric load (e/B=0). This result demonstrates that small and negative load eccentricities in the case of reinforced sand slope have a little effect on the ultimate bearing capacity because the primary failure surface from the slope side becomes deeper and larger and therefore it has a greater impact than the eccentricity one.

In Fig. 7, the variation of $i_B$ ratios with increasing eccentricities for model strip footings on the reinforced sand slope were compared with model strip footings on level reinforced sand soil experienced by Cure, Turker [10] and Turker, Sadoglu [20]. $i_B$ factor is defined as the ratio of bearing capacity of footing subjected to eccentric vertical load to that of footing subjected to a centric vertical load. As seen from Fig. 7, while the ratios show some difference until the negative load eccentricities, the ratios between the two cases are in good agreement in the case of positive eccentricities.

Fig. 8 shows the comparison between numerical and experimental load-displacement curves. Only selected load-deflection curves were presented because they virtually follow the same trend. From the graphs, it can be seen that the numerical load-displacement curves agree reasonably well with the experimental ones. The minor discrepancies between the experimental and the FEM curves are due to uncertainty in the estimation of the input parameters of the soil and the foundation and the boundary conditions adopted for both the numerical and the experimental model.

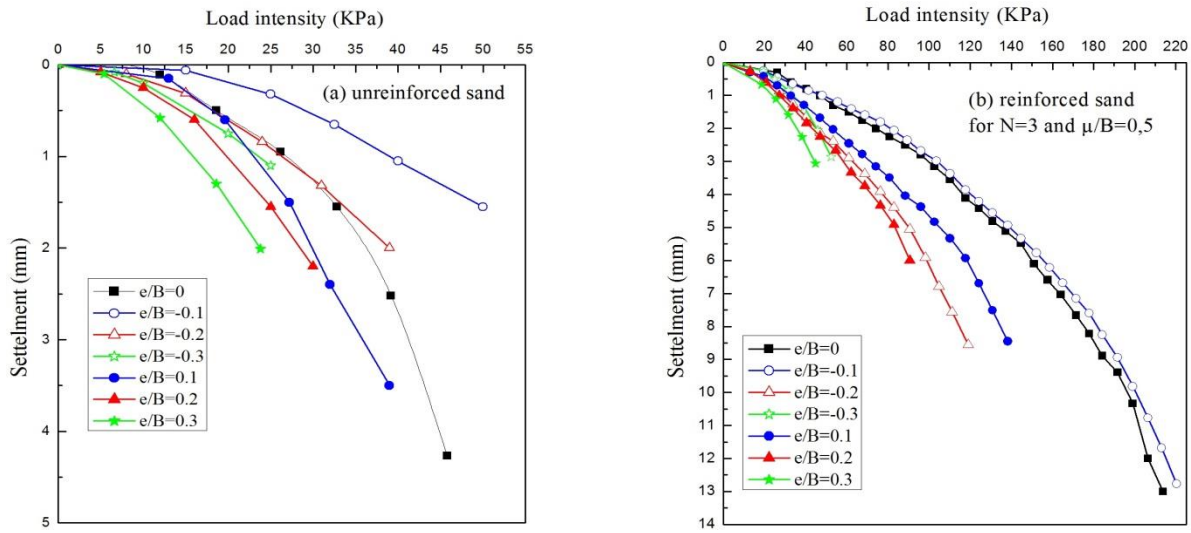


Figure 6 - Load–settlement relations obtained from experimental investigation

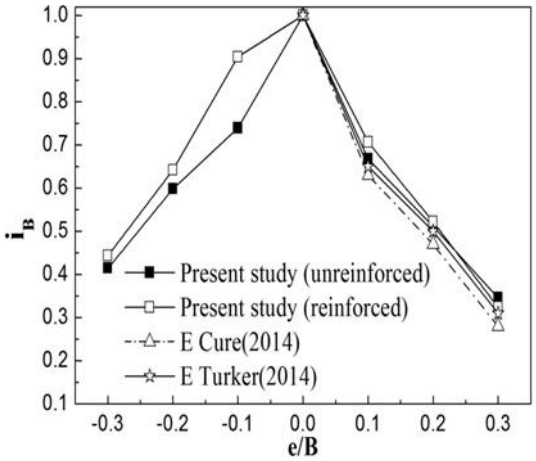


Figure 7 - Variation of $i_B$ ration with eccentricity ratio +e/B

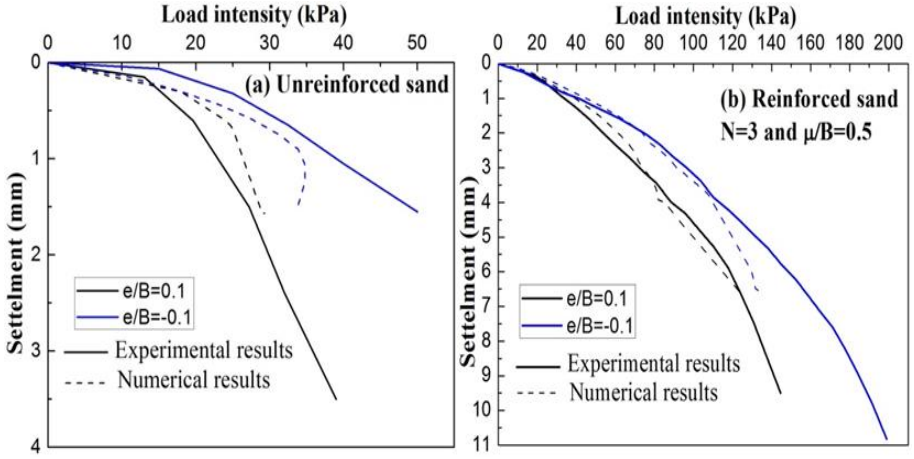


Figure 8 - Comparison between numerical and experimental results

### *4.1 Failure mechanism*

When a foundation located near a slope is loaded to failure, the zones of plastic flow in the soil on the side of the slope are smaller than those of a similar foundation on level ground and the ultimate bearing capacity is correspondingly reduced. The region above the failure surface of a shallow rough strip foundation is assumed to be divided into a central elastic zone (active zone I), a mixed shear zone (passive zone II) and a radial shear zone (III) [5, 25]. For the case of reinforced slopes, the arrangement of reinforcement has a great effect upon the critical failure surface of reinforced slopes. Actually, increasing the vertical spacing between the reinforcement layers would produce a larger depth of the reinforced zone and therefore enhances the deep footing effects which in turn improved the bearing capacity of the foundations on sloping ground. However as the ver-

tical spacing of reinforcement layers becomes larger than the half of the footing width, failure within the reinforced zone associated with a very larger softening could occur and the reinforced slope does not longer behave coherently [12]. In the current study, the adopted vertical spacing of reinforcement layers is h=0.5B which should lead to a large and deep failure surface as it is shown in Figs. 10(a), 10(b) and 10(c). It is well known from the literature that primary failure surface of the eccentrically loaded strip footing resting on horizontal ground occur at the eccentricity side and a secondary failure surface occurs at the opposite side [15]. However, the numerical and experimental results obtained in this study have shown that, regardless, the load eccentricity location relative to the slope face, the primary failure surface of the eccentrically loaded strip footing resting on unreinforced sloping ground occurs at the eccentricity side and it extends towards the slope (see Figs. 9 and 10). Therefore, the influence of the slope on the bearing capacity becomes dominant and the ultimate load decreases due to the lack of passive resistance beneath the footing. These results are similar to those obtained by Huang, Tatsuoka [12]. Fig. 10 shows that for reinforced sand slope, the primary failure surface is wider than that observed in the unreinforced soils. The tensile force resulting from the friction acting between the soil and the geogrid layers in the reinforcement decreased and the active force is reduced. The tensile force in the reinforcement enables the geogrid to resist the horizontal shear stresses that can be mobilized within the soil mass beneath the footing and transfer them to the adjacent stable layers of soil causing a wider and deeper failure. Therefore, the geogrid layers do not only increase the bearing capacity due to the development of wider failure surface but also results in broadening the contact area between soil and the rigid bottom surface of the footing. When the load eccentricity is located far away from the reinforced slope face (see Fig. 10(c)), the failure surface becomes wider and deeper than when the load eccentricities are located towards the slope face, which gives the active wedge more shear resistance. The increase in the failure surface increases the bearing capacity in the case of small and negative eccentricity (e=-0.1B) compared to that of a centered load. In this case, the geogrid play a role in increasing the bearing capacity due to a developed longer failure and greatly reduces the negative effect of the load eccentricity.

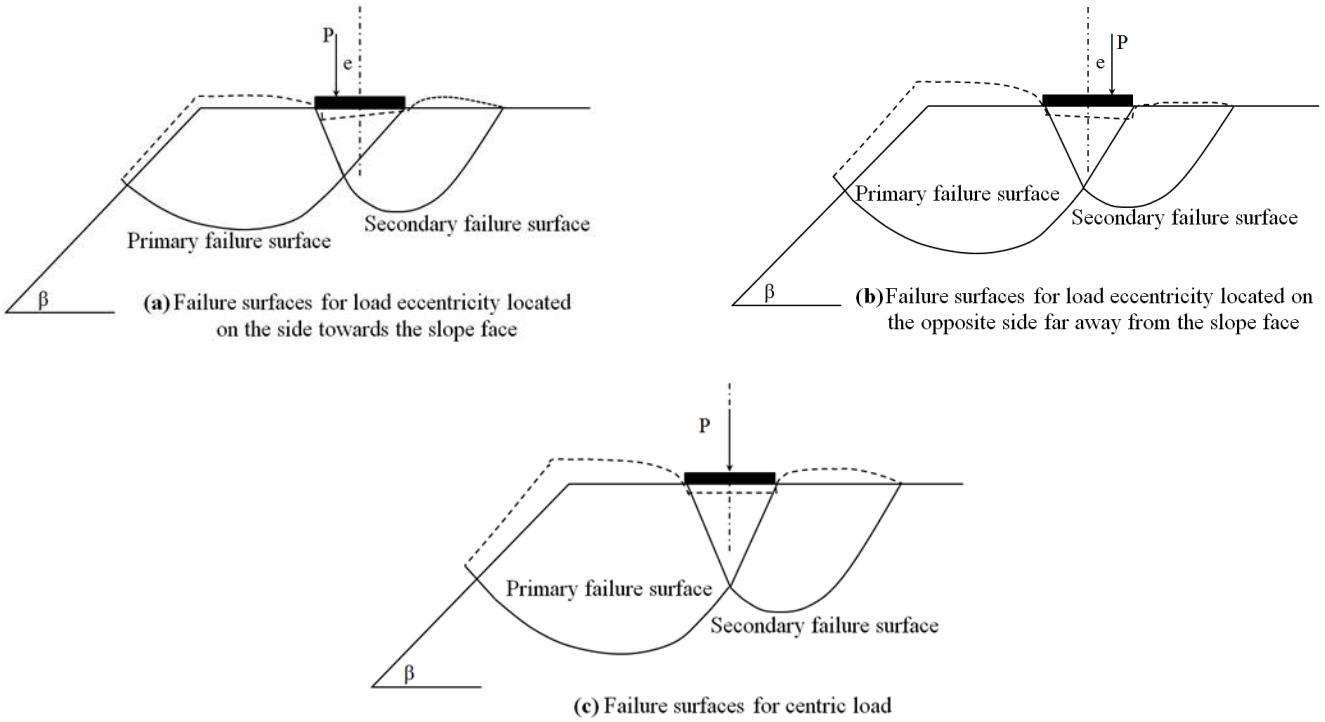


Figure 9 - Failure surfaces for unreinforced sand slope

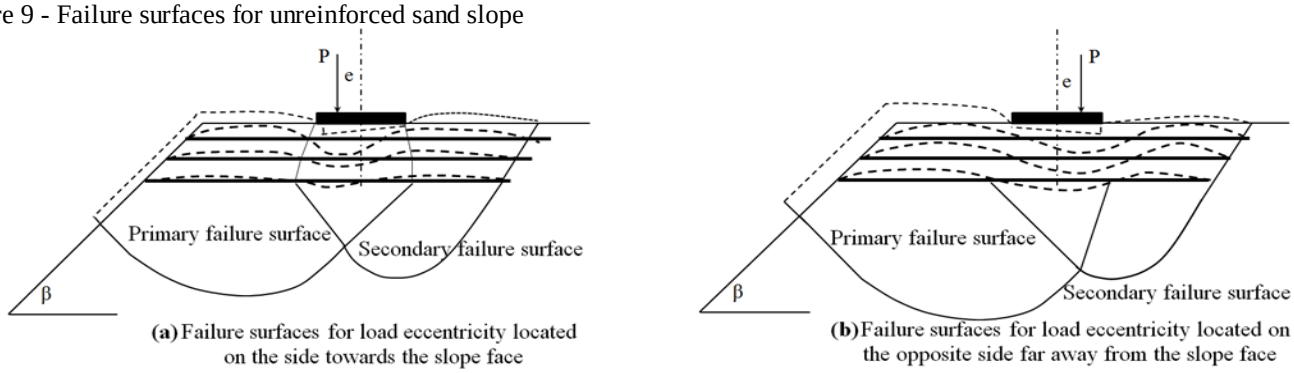

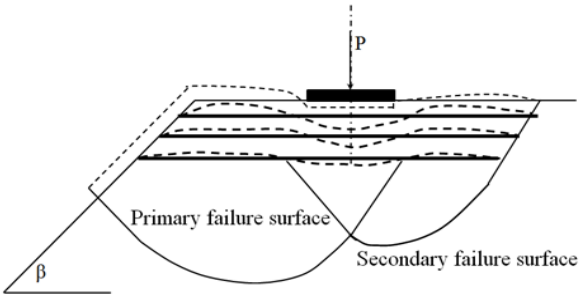


(c) Failure surfaces for centric load

Figure 10 - Failure surfaces for reinforced sand slope

### *4.2 Horizontal displacements of the footing*

To study the behavior and the failure mechanism of strip footings on unreinforced and reinforced sand slope when subjected to eccentric loading, various curves of loading versus horizontal displacement were plotted with the numerical results in Fig. 11. Fig. 11(a) shows that the horizontal displacement and the eccentricity ratio e/B have opposite signs. For negative values of e/B, the direction of the displacement was changed as the load reaches a specific value which depends on the load eccentricity. This can be explained by the progression of the slipping potential surface towards the slope, which is similar to the behavior of a foundation on a top of a slope under an inclined loading as reported by Baazouzi, Benmeddour [26]. In the case of reinforced soil with two layers of reinforcement (N=2), as illustrated in Fig. 10 b, the displacement directions was not changed for a load with eccentricity e=-0.3B. However, the variation follows the same trend as unreinforced soil for all the other values of eccentricity, meaning that the number (N=2) of reinforcement layers can balance the failure potential towards the slope for an eccentricity e=-0,3B and with an increase in the loading value. Fig. 11c illustrates the change of the horizontal displacement with the variation of loading for a reinforced soil with 4 layers of geogrids. It can be noticed that the load causing failure are increased, and the directions of the horizontal displacements was not changed for all the eccentricity values. Hence, the foundation offers a greater resistance to sliding.

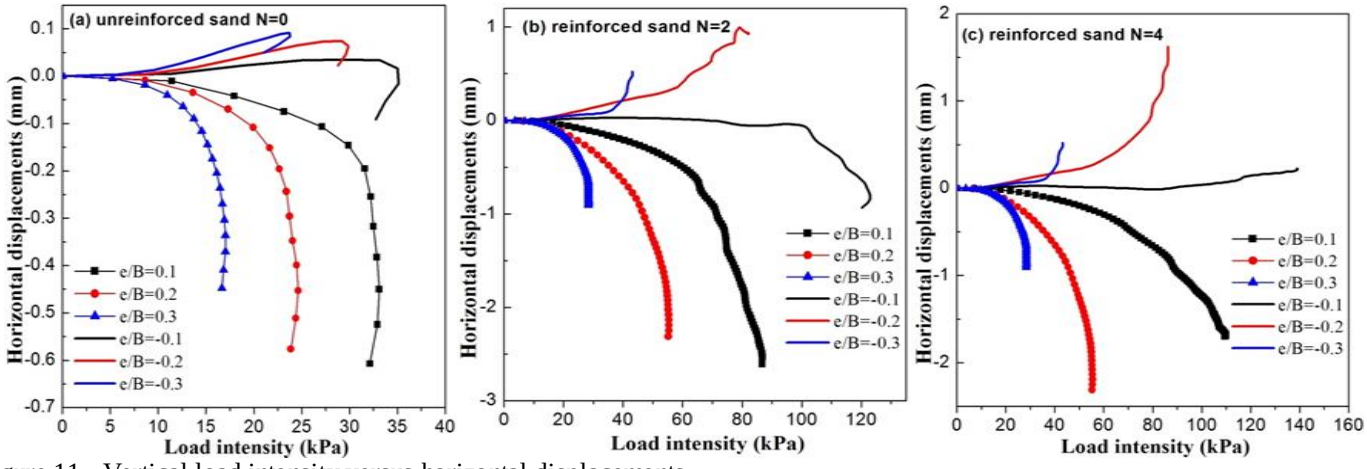


Figure 11 - Vertical load intensity versus horizontal displacements

## CONCLUDING REMARKS

1. It is proved that the location if the load eccentricity relative to the slope crest has a great effect on the footing behavior for the case of reinforced san slope
2. The optimal depth of the first layer of reinforcement is strongly linked to location of load eccentricity relative to the slope face (load eccentricity towards or far away from the slope).
3. The surface of failure, become deeper and larger for load eccentricity located far away from the slope face (e/B<0). In addition, the sliding potential of the foundation towards the slope can be balanced by using a precise number of reinforcement layers.
4. A medium agreement between the experimental and numerical results on general trend of behavior and the critical values of the geogrid parameters is observed.

ACKNOWLEDGEMENT

The authors would like to express their special thanks of gratitude to Prof “Bouassida Mounir” for their contribution in this work, who gave the golden opportunity to do this wonderful project, which also helped in doing a lot of Research.

REFERENCES

1. R.D. Purkayastha and A. Char, "Stability analysis for eccentrically loaded footings", Journal of Geotechnical and Geoenvironmental Engineering, Vol. (103), 1977, (ASCE 13014 Proceeding).
2. G.t. Meyerhof, "The bearing capacity of foundations under eccentric and inclined loads", *in Proc. of the 3rd Int. Conf. on SMFE*. 1953.
3. S. Prakash and S. Saran, "Bearing capacity of eccentrically loaded footings", Journal of Soil Mechanics & Foundations Div, Vol (4), 1971.
4. S.A. Kumar and K. Ilamparuthi, "Response of footing on sand slopes", Indian Geotechnical Society Chennai Chapter, Students Paper Competition, Vol (6), No. 6 , 2009, pp 9-12.
5. G. G Meyerhof. The ultimate bearing capacity of foundations on slopes. in Proc., 4th Int. Conf. on Soil Mechanics and Foundation Engineering, 1957.
6. A.S. Vesic, "Bearing capacity of shallow foundations", *Foundation engineering handbook*, 1975.
7. L. Bowles, "Foundation analysis and design", 1996: M c Graw-hill.
8. B.M. Das, "Principles of foundation engineering", 2015: Cengage learning.
9. S. Saran and B. Reddy, "Bearing capacity of eccentrically loaded footings adjacent to cohesionless slopes", Indian Geotechnical Journal,Vol (20), No. 2, 1990, pp 119-142.
10. E. Cure, E. Turker, and B.A. Uzuner, "Analytical and experimental study for ultimate loads of eccentrically loaded model strip footings near a sand slope", Ocean Engineering, Vol (89), 2014, pp 113-118.
11. A. Selvadurai and C. Gnanendran, "An experimental study of a footing located on a sloped fill: influence of a soil reinforcement layer", Canadian Geotechnical Journal, Vol (26), No. 3, 1989, pp 467-473.
12. C.-C. Huang, F. Tatsuoka, and Y. Sato, "Failure mechanisms of reinforced sand slopes loaded with a footing", Soils and Foundations, Vol (34), No. 2, 1994, pp 27-40.
13. K. Lee and V. Manjunath, Experimental and numerical studies of geosynthetic-reinforced sand slopes loaded with a footing, Canadian Geotechnical Journal, Vol (37), No. 4, 2000, pp 828-842.
14. C. Yoo, "Laboratory investigation of bearing capacity behavior of strip footing on geogrid-reinforced sand slope", Geotextiles and Geomembranes, Vol (19), No. 5, 2001, pp 279-298.
15. B. Moroglu, B.A. Uzuner, and E. Sadoglu, "Behaviour of the model surface strip footing on reinforced sand", 2005.
16. C. Patra, et al., "Eccentrically loaded strip foundation on geogrid-reinforced sand", Geotextiles and Geomembranes, Vol (24), No. 4, 2006, pp 254-259.
17. M.A. El Sawwaf, "Behavior of strip footing on geogrid-reinforced sand over a soft clay slope", Geotextiles and Geomembranes, Vol (25), No. 1, 2007, pp 50-60.
18. E. Sadoglu, E. Cure, B. Moroglu, B.A. Uzuner, "Ultimate loads for eccentrically loaded model shallow strip footings on geotextile-reinforced sand", Geotextiles and Geomembranes, Vol (27), No. 3, 2009, pp 176-182.
19. H.S. Al-Jubair and J.K. Abbas, "Bearing Capacity of Eccentrically Loaded Strip Footing Near The Edge of Cohesive Slope", Tikrit Journal of Engineering Sciences, Vol (16), No. 2, 2007, pp 32-48.
20. E. Turker, E. Sadoglu, E. Cure, and B. A. Uzuner, "Bearing capacity of eccentrically loaded strip footings close to geotextile-reinforced sand slope", Canadian Geotechnical Journal, Vol (51), No. 8, 2014, pp 884-895.
21. A. Choudhary, J. Jha, and K. Gill, "Laboratory investigation of bearing capacity behaviour of strip footing on reinforced flyash slope", Geotextiles and Geomembranes, Vol (28), No. 4, 2010,pp 393-402.
22. R. Brinkgreve, Plaxis, "Finite Element Code for Soil and Rock Analyses: 2D-Version 8", 2002.
23. Y. Yu, I.P. Damians, and R.J. Bathurst, "Influence of choice of FLAC and PLAXIS interface models on reinforced soil–structure interactions", Computers and Geotechnics, Vol (65), 2015, pp 164-174.
24. C.H. Trautmann and F.H. Kulhawy, "Uplift load-displacement behavior of spread foundations", Journal of Geotechnical Engineering, Vol (114), No. 2, 1988, pp 168-184.
25. J.B. Hansen, "A revised and extended formula for bearing capacity", *Danish Geotechnical Institute Bull.*,Vol (28), 1970, pp 5-11.
26. M. Baazouzi, D. Benmeddour, A. Mabrouki, and M. Mellas, "2D numerical analysis of shallow foundation rested near slope under inclined loading". Procedia engineering, 2016. Vol (143), pp 623-634.